Waggoner, A. (1976) *J. Membr. Biol. 27*, 317–334.
Waggoner, A. (1979) *Annu. Rev. Biophys. Bioenerg. 8*, 47–68.
Waggoner, A. S., Wang, C. H., & Tolles, R. L. (1977) *J. Membr. Biol. 33*, 109–140.
Westerhoff, H. V., Kamp, F., Tsong, T. Y., & Astumian, R. D. (1987) in *Mechanistic approaches to interactions of electric and electromagnetic fields with living systems* (Blank, M., & Findl, E., Eds.) pp 203–215, Plenum Press, New York.
Wrigglesworth, J. M. (1988) *Mol. Aspects Med. 10*, 223–232.
Wrigglesworth, J. M., & Nicholls, P. (1978) *FEBS Lett. 91*, 190–193.
Wrigglesworth, J. M., & Nicholls, P. (1979) *Biochim. Biophys. Acta 547*, 36–46.

Structure and Vectorial Properties of Proteoliposomes Containing Cytochrome Oxidase in the Submitochondrial Orientation†

Chris E. Cooper‡ and Peter Nicholls*
Department of Biological Sciences, Brock University, St. Catharines, Ontario, Canada L2S 3A1
Received September 14, 1989; Revised Manuscript Received December 18, 1989

ABSTRACT: Cytochrome oxidase proteoliposomes were prepared from bovine heart oxidase. Size distributions determined by quasi-elastic light scattering (QELS) showed that there was a small population of large vesicles (120–200-nm diameter) and a large population of small vesicles (50–100-nm diameter). Trapping cytochrome *c* inside the proteoliposomes did not significantly alter this size distribution. Separation of the vesicles by gel filtration, however, revealed that the cytochrome *c*/cytochrome *a* ratio is higher in the larger vesicles. Internally trapped cytochrome *c* can be reduced by the membrane-permeable reductants 2,3,5,6-tetramethyl-*p*-phenylenediamine (DAD) or *N,N,N′,N′*-tetramethyl-*p*-phenylenediamine (TMPD). Respiration on internal cytochrome *c* generated a membrane potential of 53 mV (positive inside) and a pH gradient of 0.2 (acid inside) as monitored by the optical probes oxonol V and pyranine, respectively. But the true magnitude of these gradients in individual proteoliposomes is complicated by vesicle heterogeneity. The membrane potential increased biphasically with increasing concentration of reductant. Ionophore sensitivity was higher for the "low K_m" phase, and respiration became increasingly uncoupled as the reductant concentration was increased. These findings are consistent with a kinetic heterogeneity such that vesicles respiring at lower reductant concentrations generate a higher proton motive force than those with a larger K_m. The steady-state internal acidification induced by turnover of the internally facing enzyme is probably maintained by both cytochrome oxidase proton translocation and a $TMPD^+/H^+$ antiport present in these vesicles [Cooper, C. E., & Nicholls, P. (1987) *FEBS. Lett. 223*, 155–160].

Cytochrome *c* oxidase vesicles capable of respiring on internally trapped cytochrome *c* (*c*-loaded COV)[1] can be prepared simply by the preaddition of cytochrome *c* to the reconstitution medium (Racker & Kandrach, 1971; Nicholls et al., 1980; Cooper & Nicholls, 1987). The internally facing enzyme in such *c*-loaded vesicles turns over upon the addition of membrane-permeable reductants such as phenazine methosulfate (Racker & Kandrach, 1971) or TMPD (Cooper & Nicholls, 1987). An apparently low turnover number for the enzyme respiring on internal cytochrome *c* is due to a high K_m for TMPD (Cooper & Nicholls, 1987). In the aerobic steady state, cytochrome *c* loaded COV accumulate $TMPD^+$ (Würster's Blue); the effects of ionophores on the $TMPD^+$ level provide indirect evidence that cytochrome oxidase respiring on internal cytochrome *c* generates a $\Delta\mu H^+$ of an orientation opposite to that generated by enzyme respiring on external cytochrome *c* (Cooper & Nicholls, 1987; Nicholls et al., 1988a).

However, the response of internally facing enzyme to ionophores is poor (Nicholls et al., 1980; Cooper & Nicholls, 1987), and some authors have suggested that internally facing enzyme molecules do not incorporate successfully into proteoliposomes (Madden et al., 1987). We therefore decided to analyze the structure of *c*-loaded COV to determine whether addition of cytochrome *c* causes any morphological changes to the vesicles; we have also used $\Delta\mu H^+$-sensitive probes to measure directly the proton motive force that is generated by the oxidation of internal cytochrome *c*. The results show that cytochrome *c* loaded COV are structurally indistinguishable from standard COV but that they generate a significant proton motive force of an orientation opposite to that generated in such standard COV.

Materials and Methods

Cytochrome *c* oxidase was purified from beef hearts according to the procedure of Kuboyama et al. (1972) with Tween 80 substituting for Emasol as the final detergent. Liposomes and cytochrome oxidase proteoliposomes (COV) were prepared by the sonication technique as described previously (Proteau et al., 1983). Cytochrome *c* loaded COV were also made by sonication, and the excess, external, cytochrome

† Supported by Canadian Natural Sciences and Engineering Research Council Operating Grant A-0412 to P.N. and an Ontario Graduate Scholarship to C.E.C.
* To whom correspondence should be addressed.
‡ Present address: Biochemistry Section, Division of Biomolecular Sciences, King's College, Campden Hill Rd., Kensington, London W8 7AH, U.K.

[1] Abbreviations: BTPP, *n*-butyltriphenylphosphonium; COV, cytochrome *c* oxidase proteoliposomes; *c*-loaded COV, COV containing entrapped cytochrome *c*; DAD, 2,3,5,6-tetramethyl-*p*-phenylenediamine; $diSC_3$-5, 3,3′-dipropylthiodicarbocyanine; FCCP, carbonyl cyanide *p*-(trifluoromethyl)phenylhydrazone; oxonol V, bis[3-phenyl-5-oxoisoxazol-4-yl]pentamethineoxonol; pyranine, trisodium 8-hydroxy-1,3,6-pyrenetrisulfonate; QELS, quasi-elastic light scattering; TMPD, *N,N,N′,N′*-tetramethyl-*p*-phenylenediamine.

0006-2960/90/0429-3865$02.50/0

c was subsequently removed on a Sephadex CM-25 cation-exchange column (Cooper & Nicholls, 1987). The internal medium in all vesicle preparations was 50 mM potassium phosphate, pH 7.4.

For determinations of internal pH, the pH probe pyranine was trapped inside the liposomes by adding up to 5 mM to the phospholipid suspension before mechanical mixing (Nicholls et al., 1988a). The external pyranine in standard COV preparations is normally removed by passage through G-25 Sephadex; the green, fluorescent vesicles pass in the void volume and the external probe is retarded (Singh & Nicholls, 1986). For cytochrome *c* loaded COV, passage through Sephadex CM-25 did not result in separation of external pyranine. The positively charged, external, cytochrome *c* was bound to the negatively charged beads and remained at the top of the column, but the negatively charged pyranine did not enter the beads and traveled with the proteoliposomes in the void volume. It was therefore necessary to pass the vesicles through a Sephadex G-25 column prior to the Sephadex CM-25 to remove the external pyranine and cytochrome *c* in successive stages.

Freeze-fracture electron microscopy was used to compare the size and shape of COV and *c*-loaded COV. The vesicle preparations were diluted to a concentration of 5 mg of phospholipid/mL with 50 mM potassium phosphate, pH 7.4; they were then rapidly spray-freezed without cryoprotectant on standard Balzers equipment (Rand et al., 1985; Kachar et al., 1986). Freeze fracturing was done with a Balzers 400T apparatus (Hudson, NY) using both cleaving and quartz crystal monitored shadowing (45°) and replicating at 5×10^{-8} mbar and −150 °C. The size distribution of the vesicles was determined by quasi-elastic light scattering (Herb et al., 1987). The laser configuration employed was as described in Hallett et al. (1989). Particle size analysis for intensity and number distributions was essentially as described for solid spheres in Hallett et al. (1989). However, the algorithm was modified (Hallett, unpublished results) as it was assumed that the vesicles were hollow spheres.

Vesicle size was also determined by gel filtration. Pyranine and cytochrome *c* loaded COV were passed down a Sepharose 2B column (exclusion limit 4×10^7 Da). The flow rate was 4 min/mL. A series of 2-mL fractions was taken and analyzed for light scattering, cytochrome *c*, cytochrome aa_3, and pyranine content as described under Results.

Oxygen consumption was measured polarographically by using a Clark oxygen electrode (Yellow Springs Instruments) attached to a Brock University electronics shop polarizing box and a Perkin-Elmer 56 recorder. The nonenzymatic autoxidation rate was subtracted from the total rates to give the corrected turnover numbers.

The change in pyranine absorbance with time was monitored at 470 minus 656 nm by using an Aminco DW-2 spectrophotometer operating in dual-beam mode with a thermostatically controlled cuvette holder. All experiments were carried out at 30 °C.

Mixed phospholipids of the "asolectin" type (type IV-S, phosphatidylcholine), Ascorbate (L-ascorbic acid, sodium salt), cytochrome *c* (horse heart, type VI), TMPD dihydrochloride, and valinomycin were all obtained from Sigma. Nigericin was from Calbiochem, DAD from Polyscience, and oxonol V from Molecular Probes. FCCP was the kind gift of Dr. P. G. Heytler (Du Pont).

Results

Freeze-fracture electron microscopy (Figure 1) revealed that cytochrome oxidase containing proteoliposomes are spherical

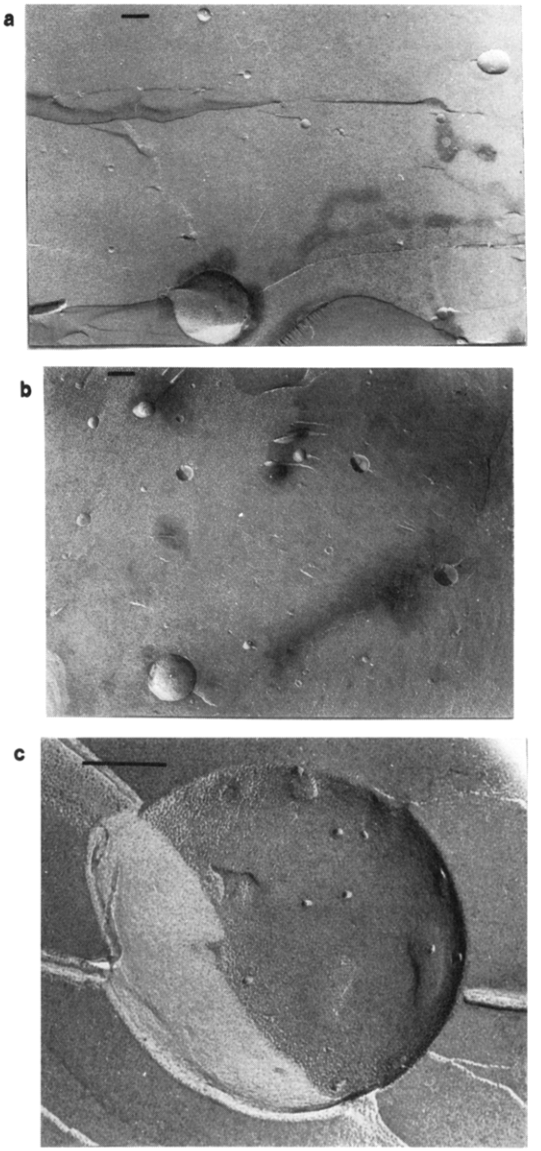

FIGURE 1: Electron micrographs of COV and cytochrome *c* loaded COV. Freeze-fracture preparations were made as described under Materials and Methods. Scale bar = 100 nm. (a) COV; (b) *c*-loaded COV; (c) enlargement of a single COV.

but show a significant heterogeneity in vesicle size, both in the presence (Figure 1a) and in the absence (Figure 1b) of entrapped cytochrome *c*. The two preparations contained vesicles whose diameters ranged from 20 to 200 nm, with an occasional very large (400 nm) vesicle (Figure 1c). This is in good agreement with the size distribution calculated from similar micrographs of sonicated vesicles by Wrigglesworth (1985). No differences could be seen between the vesicles in the micrographs of COV and of *c*-loaded COV.

The presence of protein in these vesicles is indicated by "bumps" or "hollows" where the fracture plane passes over or under an enzyme molecule embedded in the membrane. None of the very small (20 nm) vesicles contained protein, but slightly larger vesicles frequently contained one enzyme molecule. Figure 1c shows a single large vesicle containing at least 10 enzyme molecules. It is not certain which way the enzyme molecules are facing in these images, but clearly there is the potential for large vesicles to contain both inwardly and outwardly facing oxidase molecules.

Larger particles scatter light more effectively than smaller ones. Consequently, there is a decrease in light scattering during vesicle formation by sonication (Wrigglesworth, 1988).

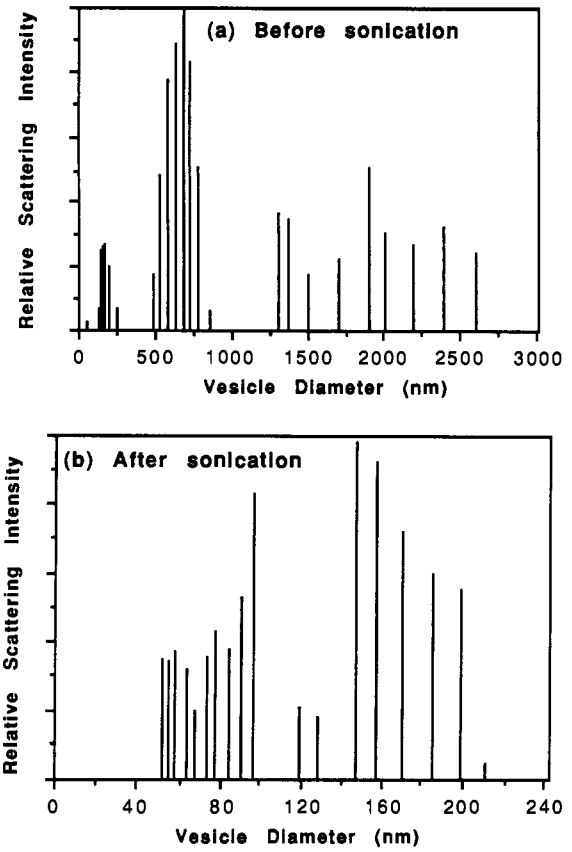

FIGURE 2: Effect of sonication on the size of phospholipid vesicles: QELS assay. Light scattering measurements were performed as described under Materials and Methods. (a) 0.4 mg/mL protein-free phospholipids were dispersed in 50 mM potassium phosphate, pH 7.4. (b) 5 mg/mL protein-free phospholipid, after 12 min of sonication in 50 mM potassium phosphate, pH 7.4.

To quantify vesicle size by use of information from light scattering, a more sophisticated technique is required than the monitoring of absorbance change at a single wavelength. Quasi-elastic light scattering (QELS) provides a rapid and noninvasive measure of size distribution in populations of particles with a known and homogeneous shape. If it is assumed that the vesicles are perfect spheres, an intensity distribution such as that shown in Figure 2 is obtained for enzyme-free vesicles before and after sonication. Prior to sonication there is a large variation in vesicle diameter, from a minimum of about 50 nm to a maximum of up to 2.5 μm (Figure 2a). The average diameter decreases dramatically after sonication (Figure 2b). However, there appear to be at least two distinct populations of vesicle, one with a size range from 50 to 100 nm and the other with a size range from 120 to 200 nm.

Figure 3 shows the results obtained from an analogous QELS study of COV and *c*-loaded COV. Parts a and b of Figure 3 reveal size distributions almost identical with those observed with enzyme-free vesicles (Figure 2). No significant difference is caused by cytochrome *c*. This suggests that any structural heterogeneities in *c*-loaded COV, which may be responsible for the high K_m for TMPD (Cooper & Nicholls, 1987), must also be present in COV.

The distributions shown in Figures 2 and 3 are intensity distributions. To compare these distributions to those observed from counting vesicles in freeze-fracture electron micrographs, it is necessary to convert this intensity distribution to a number distribution. An efficient conversion algorithm has recently been developed for both solid (Hallett et al., 1989) and hollow (Hallett, unpublished results) spheres. As scattering is proportional to the square of the particle mass and hence the sixth power of the radius (Hallett et al., 1989), it is clear that the

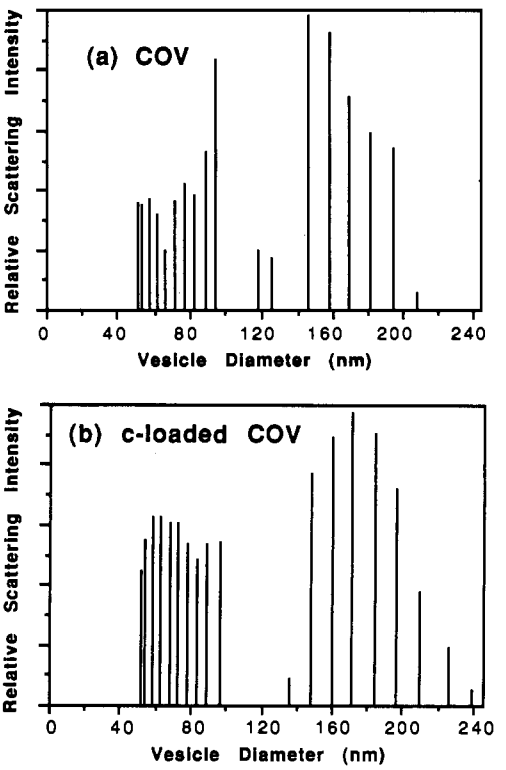

FIGURE 3: Effect of sonication on the size of cytochrome oxidase containing proteoliposomes: QELS assay. Proteoliposomes were prepared as described under Materials and Methods (12-min sonication time). Light scattering measurements were determined in 50 mM potassium phosphate, pH 7.4: (a) 5 mg/mL COV; (b) 5 mg/mL *c*-loaded COV.

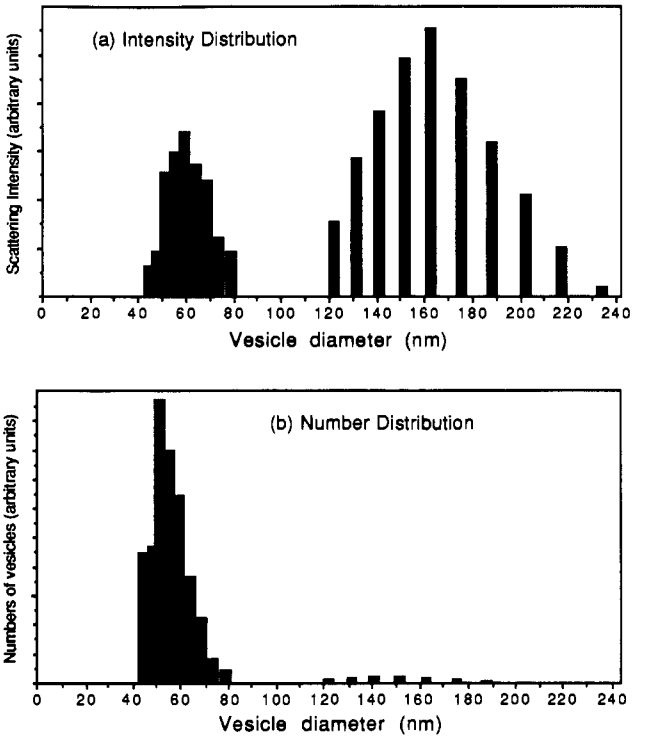

FIGURE 4: Comparison of intensity and number distributions for cytochrome oxidase proteoliposomes as determined by QELS. COV (1.2 mg/mL) (after 12 min of sonication) in 50 mM potassium phosphate, pH 7.4. Vesicle size was compared to the relative light scattering intensity (a) and the relative number of vesicles (b) by using quasi-elastic light scattering as described under Materials and Methods.

Table I: Comparison of Trap Volumes and Cytochrome Contents of Small and Large *c*-Loaded COV Separated on a Sepharose 2B Column[a]

property	vesicle fraction	
	1–10 (large)	11–24 (small)
%[b] light scattering	49.5	51.5
% pyranine	56	44
% cytochrome *c*	38	62
% cytochrome *a*	16	84
cyt *c*/cyt *a* ratio	5.19	1.64

[a] Data obtained from Figure 5. [b] % = percent of total light scattering, pyranine etc., contained in fraction.

number distribution will have a much smaller contribution from the larger vesicles. This is shown in Figure 4, where the intensity and number distributions are compared for COV. The calculated number distribution observed, with a large number of small vesicles and a small number of large vesicles, is in good agreement with that determined from electron micrographs of sonicated COV (Wrigglesworth, 1985).

A third method used to measure vesicle size was that of gel filtration on a Sepharose 2B column. This has the advantage that individual vesicle populations are separated and thus can be analyzed for cytochrome *a*, cytochrome *c*, and trap volume (by use of the pH probe pyranine) as well as for the vesicular size. Light scattering was monitored by using the absorbance difference between 350 and 371 nm, a wavelength pair relatively unaffected by absorbance changes due to cytochrome or pyranine. Similar experiments with dialyzed vesicles had previously shown a small fraction consisting of mostly large lipid aggregates and a larger fraction of enzyme-containing vesicles (Wrigglesworth, 1985). The use of Sepharose 4B allowed the additional separation of a population of very small vesicles (20-nm diameter), which contain virtually no cytochrome oxidase molecules (Casey et al., 1984).

In contrast to these reports, and in agreement with the results presented in Figures 2–4, our preparations of sonicated vesicles showed a clearly bimodal size distribution; both populations contained significant amounts of cytochrome oxidase, cytochrome *c*, and pyranine (Figure 5a,b). A small amount of pyranine (presumably free material released from vesicles) elutes after the two sets of vesicles. Either pyranine leaks very slowly from the vesicles or there is an occasional lysis of vesicles that allows pyranine to appear in the external solution.

Table I summarizes the relative proportions of cytochrome *c*, cytochrome *a*, pyranine, and light scattering in the two vesicle populations. The amount of light scattering is approximately equal in the two populations, suggesting that the populations separated are the same as those observed in the QELS experiments (Figures 2–4). The amount of pyranine entrapped in the two fractions is approximately the same, which suggests that their trap volumes are also similar. However, proportionately more cytochrome *a* and cytochrome *c* are found in the smaller vesicles. If one compares the amounts of the two cytochromes relative to the trap volumes, it can be concluded that cytochrome *a* content is drastically reduced in the larger vesicles while cytochrome *c* is more evenly distributed.

The pH gradient in cytochrome oxidase proteoliposomes may be measured by fluorescence changes in the pH probe pyranine (Singh & Nicholls, 1986; de Vrij et al., 1986; Nicholls et al., 1987). However, $TMPD^+$ quenching of the pyranine fluorescence signal makes it difficult to quantify the gradient in *c*-loaded COV (Nicholls et al., 1988a; Cooper, 1989). The $TMPD^+$ spectrum is very broad, with significant

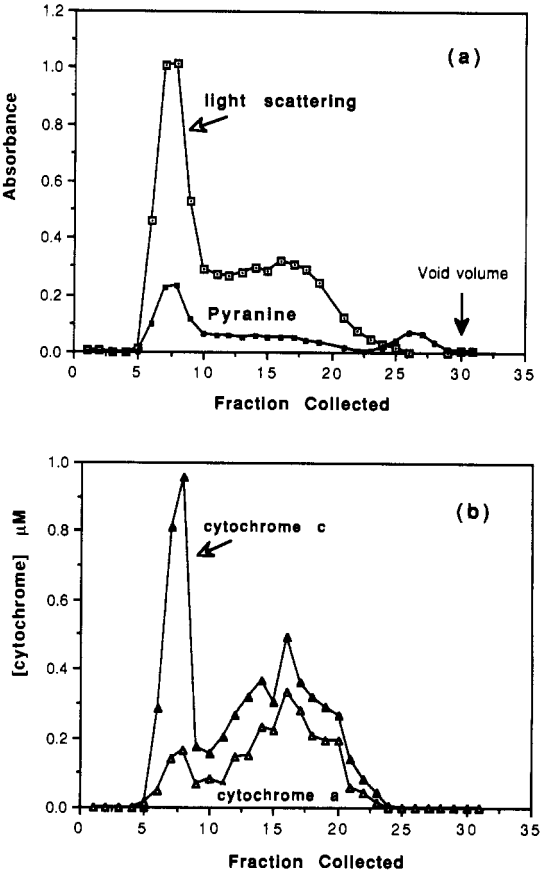

FIGURE 5: Separation of different sizes of *c*-loaded COV by column chromatography on Sepharose 2B. Pyranine- and *c*-loaded COV were passed through a Sepharose 2B column as described under Materials and Methods. (a) Vesicle size was monitored by following the light scattering difference in the absolute spectra, using the wavelength pair 350–471 nm. Pyranine content was measured by following the difference in the absolute spectra at 455–471 nm. As an extra control pyranine content was assayed by monitoring the difference in the wavelength pair 470–500 nm after the addition of 2 mM KOH in the presence of 2 μg/mL nigericin. The elution pattern observed was identical with that seen in the figure. (b) Cytochrome *c* content and cytochrome *a* content were measured by monitoring the changes in the wavelength pairs 550–540 and 605–630 nm, respectively, after the addition of 2 mM sodium ascorbate and 0.3 mM TMPD to the vesicles in the presence of 100 μM KCN and 2 μg/mL nigericin.

absorbance from 450 to 660 nm. As pyranine absorbs at 460 nm and fluoresces at 510 nm, the quench observed could be due to $TMPD^+$ absorbance of either the excitation or the emitted light.

The broad $TMPD^+$ spectrum also makes it difficult to use alternative pH probes (e.g., phenol red). However, Figure 6 shows that when the pyranine *absorbance* is monitored at 470–656 nm, there is relatively little interference from $TMPD^+$. In the presence of valinomycin and FCCP only very small changes are seen at this wavelength pair (Figure 6a); these may be due to interference from the Soret absorbance of cytochrome aa_3 rather than to $TMPD^+$. In the absence of any ionophores (Figure 6b) there is a slow rise to a steady-state gradient of about 0.15 ΔpH (acid inside), followed by a subsequent slow collapse upon anaerobiosis. The addition of low levels of valinomycin (Figure 6c) increases both the rate of formation and the extent of the pH gradient, as has been reported for COV (Nicholls et al., 1987).

The formation of a membrane potential in *c*-loaded COV can be measured by using the dye oxonol V (Cooper et al., 1990). Figure 7 shows the variation in apparent membrane potential in *c*-loaded COV as reductant concentration is increased. In the presence of nigericin, there is a rapid rise to

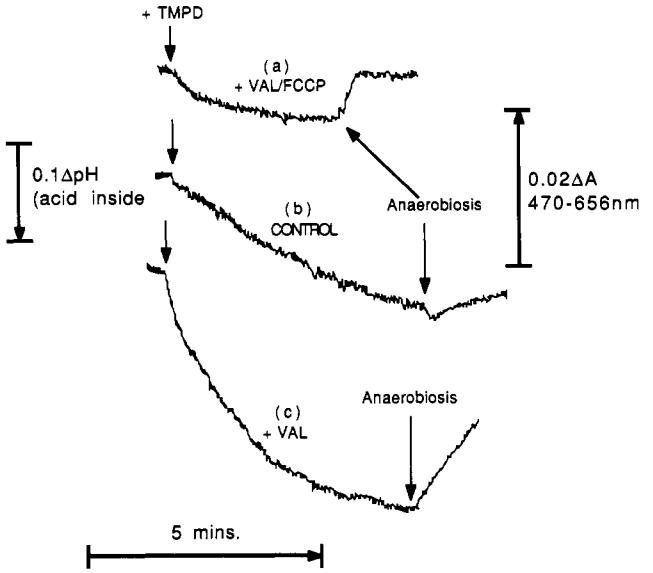

FIGURE 6: Effect of internal turnover on ΔpH in cyt *c* loaded COV as measured by pyranine absorbance changes. *c*-loaded COV (0.17 μM aa_3, 2.8 mg/mL phospholipid) in 50 mM potassium phosphate, 5 mM sodium ascorbate, pH 7.4. Turnover of internal cyt *c* was initiated by the addition of 0.3 mM TMPD at the indicated times: (a) +100 ng/mL valinomycin and 1 μM FCCP; (b) control (no ionophores); (c) +100 ng/mL valinomycin. The decrease in pyranine absorbance at 470–656 nm (indicating acidification of the vesicle interior) was calibrated with passive pH pulses in the presence of valinomycin and FCCP.

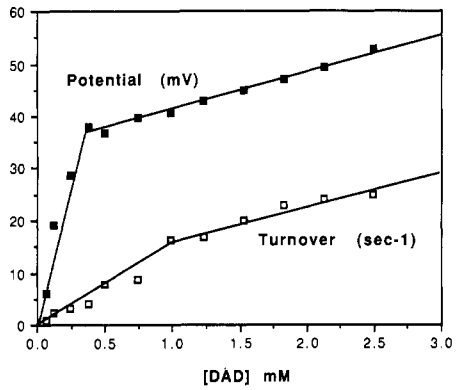

FIGURE 7: Effect of the concentration of DAD on membrane potential in *c*-loaded COV. Potassium phosphate (50 mM), pH 7.4, 5 μM oxonol V, *c*-loaded COV (1.7 mg/mL phospholipid, 38 nMaa_3), 100 ng/mL nigericin, 5 mM sodium ascorbate. The concentration of DAD was varied and the steady-state membrane potantial (■) calculated from the absorbance change at 640–690 nm calibrated by using passive gradients of potassium in the presence of valinomycin as described in Cooper (1989). The turnover of the vesicular enzyme was obtained in a parallel experiment using an oxygen electrode under the same conditions (□).

a value of 38 mV at low DAD levels and then a slower rise to 53 mV at the highest levels of DAD used (2.5 mM). These two phases are possibly linked to the two phases of turnover shown in parallel oxygen electrode experiments under similar conditions [see also Cooper and Nicholls (1987) and Cooper (1989)].

As most membrane potential formation is associated with vesicles with a low apparent K_m for DAD (Figure 7), it was necessary to test the sensitivity of the internal flux to ionophores over a range of reductant concentration. Cytochrome *c* loaded COV also contain externally facing enzyme molecules (Nicholls et al., 1980). It is thus possible to compare internal and external respiratory control ratios by using the same batch of vesicles over the same turnover range. Internal turnover

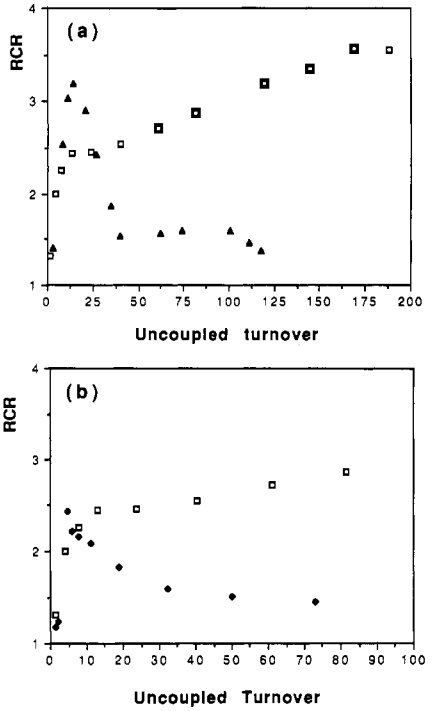

FIGURE 8: Effect of turnover on the respiratory control ratio in *c*-loaded COV. *c*-loaded COV (53 nM aa_3 for rates above 10 s^{-1} and 133 nM aa_3 for rates below 10 s^{-1}) were dispersed in 50 mM potassium phosphate, pH 7.4, containing 5 mM sodium ascorbate. Internal and external fluxes ±1 μM FCCP and/or 0.1 μg/mL valinomycin were calculated. The uncontrolled rate was divided by the controlled rate to give the respiratory control ratio (RCR) as a function of the uncontrolled turnover. The maximal (uncontrolled) turnover (μMe⁻ μM aa_3^{-1} s^{-1}) is expressed in terms of total enzyme concentration, although vesicular enzyme orientation was 50:50 (internal:external). (a) Oxidase activity was varied by increasing [TMPD] from 0.01 to 4 mM (▲) or [cytochrome *c*] from 0.33 to 215 μM (□). (b) Oxidase activity varied by increasing [DAD] from 0.025 to 2 mM (◆) or [cytochrome *c*] as in (a) (□).

was increased by the addition of TMPD or DAD (in the absence of external cytochrome *c*) and external turnover by increasing external cytochrome *c* concentration (in the absence of membrane-permeable reductants).

Figure 8a shows that the respiratory control induced with externally facing enzyme always increases with uncontrolled flux; the increase is steep at first and then more gradual. But the "internal" RCR rises to a maximum of 3.2 (at 0.08 mM TMPD) and then drops to a minimum of 1.4 (at 4 mM TMPD). This effect is not TMPD specific; Figure 8b shows that a similar result is obtained by using DAD. A maximum respiratory control ratio in this case of 2.4 is reached at a DAD concentration of 0.05 mM.

Discussion

Three different procedures, electron microscopy, light scattering, and gel filtration, have each shown significant size heterogeneity in the *c*-loaded COV following sonication; at least two distinct populations are present in our preparations. As shown by electron microscopy, the vesicles are spherical and many, but not all of them, contain cytochrome oxidase molecules. Freeze-fracture electron microscopy cannot show the number of lamellae per vesicle. But by comparing the results of freeze-fracture and transmission electron microscopy on the same vesicle preparations, Nicholls (1983) and Wrigglesworth (1985, 1988) were able to show that only the large vesicles seen in sonicated COV preparations are multilamellar; the smaller sonicated COV are unilamellar, as are nearly all the vesicles in dialyzed COV preparations. The presence in

the cytochrome *c* loaded COV of numerous large vesicles containing many oxidase molecules (Figure 1c) supports our earlier hypothesis (based upon the $TMPD^+$ steady-state behavior) that individual vesicles may form containing fully functional oxidase molecules of both orientations (Cooper & Nicholls, 1987).

Bayerl et al. (1988) have used QELS to study the size of vesicles prepared by sonication of equimolar amounts of dimyristoylphosphatidylcholine and dipalmitoylphosphatidylcholine. They suggest that a small population of large vesicles (>100-nm diameter) is the result of aggregation. However, this seems an unlikely explanation for the bimodal size distribution seen in the present work (Figures 2–4); the electron microscopy [see Figure 1 and Wrigglesworth (1988)] clearly shows that individual vesicles can be formed greater than 100 nm in diameter. The size distributions determined by QELS agree satisfactorily with those obtained by counting images in negatively stained electron micrographs (Wrigglesworth, 1985). Both methods show a bimodal distribution [cf. Figure 2 and Wrigglesworth (1985)].

Chromatography (Table I) shows that the cytochrome *a* content is markedly reduced in the larger vesicles while cytochrome *c* is more evenly distributed. This difference is even greater if cytochrome *a* content is calculated in terms of trap volume. If cytochrome oxidase only inserts into the outer bilayer of multilamellar vesicles (Wrigglesworth, 1985), then such lower levels of cytochrome *a* in the large vesicles would be expected. Cytochrome *c* may enter some of the inner lamellar spaces, and pyranine can probably enter them all. In consequence (cf. Table I) the cytochrome *c*:cytochrome oxidase ratio declines as the vesicles decrease in size.

Vesicle heterogeneity also leads to variations in the generation of potential and pH gradients. In the presence of nigericin, $\Delta\Psi$ in *c*-loaded COV increases with DAD concentration. The $\Delta\Psi$ in individual vesicles may nevertheless vary because the probe can only give an average signal at each potential. The results with varying levels of TMPD and DAD (see Figure 8) are consistent with the membrane potential heterogeneity shown in Figure 7. The low K_m activity appears to be controlled and the high K_m activity uncontrolled. If uncontrolled vesicles are accessed preferentially at high DAD concentrations, then the potentials involved will be underestimated. Thus, it is *not* correct to say that the respiratory control ratio of 2.4 at 0.05 mM DAD (Figure 8) is caused by a $\Delta\Psi$ of only 5 mV (Figure 7).

The tightly controlled internally facing enzyme must be associated with vesicles that are relatively proton impermeable. Indeed, for an equivalent flux, its respiratory control is *higher* than that shown by externally facing enzyme. TMPD and DAD both reduce cytochrome *c* more rapidly than does ascorbate, and therefore the flux per unit quantity of enzyme will be higher with TMPD or DAD than with ascorbate alone.

Two possible explanations for the decrease in ionophore sensitivity of internally facing enzyme at high [TMPD] or [DAD] are as follows.

(i) The active proteoliposomes are unusually permeable to protons. Increasing external cytochrome *c* concentration always *increases* the control ratio. Therefore, leaky vesicles must also have a high K_m(app) for TMPD. These vesicles may thus contain cytochrome *c* bound so that it requires high TMPD levels for reduction *and* increases permeability. As internal $TMPD^+$ levels increase with increasing [TMPD] (Cooper, 1989) and may diminish control, this would explain why such a decrease is seen only when flux is varied with TMPD, not with ascorbate, but it would still not explain why increasing

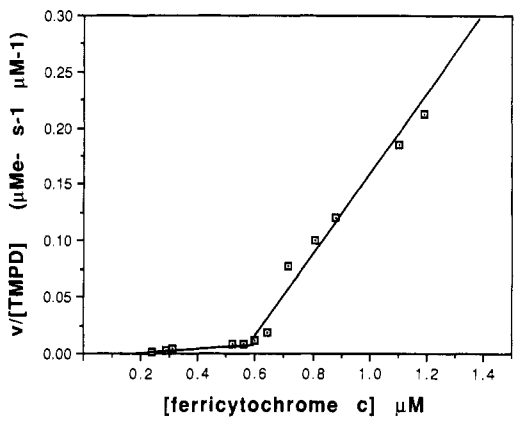

FIGURE 9: Rate of reduction of cytochrome *c* by TMPD in cytochrome *c* loaded COV. Data are taken from Cooper and Nicholls (1987). The spectrophotometer cuvettes contained cytochrome *c* loaded COV (0.22 μM cytochrome aa_3) in 50 mM potassium phosphate, pH 7.4, plus 5 mM ascorbate, 1.7 μM FCCP, and 167 ng/mL valinomycin. The steady-state level of ferricytochrome *c* was monitored at 550–540 nm. The TMPD concentration was varied from 0 to 10 μM. The lines represent least-squares fits to the first six and the last seven points. The slopes of these lines are equal to the apparent rate constants (k, k') for the reduction of cytochrome *c* by TMPD in COV: at low [ferricytochrome *c*], $k = 2.1 \times 10^4\ M^{-1}\ s^{-1}$ [incorrectly reported as $2 \times 10^5\ M^{-1}\ s^{-1}$ in Cooper and Nicholls (1987)]; at high [ferricytochrome *c*], $k' = 3.3 \times 10^5\ M^{-1}\ s^{-1}$.

[DAD] also decreases control.

(ii) The kinetics change at high TMPD levels. Figure 9 shows our previous data (Cooper & Nicholls, 1987), replotted as $J_{ox}/[TMPD]$ against $[c^{3+}]$. If we have

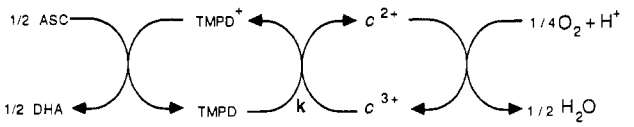

(Asc=Ascorbate, DHA= dehydroascorbate)

where $k[TMPD][c^{3+}] = J_{ox}$ (steady-state rate of oxygen consumption) and $J_{ox}/[TMPD] = k[c^{3+}]$, then a plot of $J_{ox}/[TMPD]$ against $[c^{3+}]$ will be a straight line passing through the origin, with the slope k. Two distinct slopes are, however, observed in Figure 9. These correspond to the two phases of cyt *c* oxidation (Figure 7; Cooper & Nicholls, 1987). Values for k of $3.3 \times 10^5\ M^{-1}\ s^{-1}$ in the low K_m phase and $2.1 \times 10^4\ M^{-1}\ s^{-1}$ in the high K_m phase compare with rate constants of $1.3 \times 10^5\ M^{-1}\ s^{-1}$ for TMPD reduction of oxidase-bound cytochrome *c* and $3.5 \times 10^4\ M^{-1}\ s^{-1}$ for cytochrome *c* in solution (Hill & Nicholls, 1980). At low [TMPD] enzyme-bound cytochrome *c* is being reduced; at higher [TMPD] the cytochrome *c* being reduced is in solution. Reduction of oxidase-bound *c* also increases turnover because it can occur without cytochrome *c* dissociation (Ferguson-Miller et al., 1978). Heterogeneity (Figures 8 and 9) is thus explained kinetically; as the flux per enzyme equivalent is lower at high [TMPD], a smaller proton motive force is generated per vesicle. Just as there is almost no control of externally stimulated flux at very low concentrations of cytochrome *c* (Figure 8), the differences in rate constants may reflect the cytochrome *c*:cytochrome oxidase ratios. The large vesicles also have a higher *c*:*a* ratio, and the kinetic heterogeneity may thus be related to the structural heterogeneity.

Recently Murphy and Brand (1987) have questioned whether cytochrome oxidase pumps protons at high proton motive force. Both limited turnover (Cooper, 1989) and steady-state experiments (Nicholls et al., 1988a; Figure 6, this paper) show that *c*-loaded COV translocate protons into the

vesicle when respiring with TMPD as substrate. Such internal acidification in submitochondrial particles has been taken as evidence for steady-state proton translocation by the oxidase (Wikstrom & Krab, 1979). If all the scalar protons from ascorbate oxidation or oxygen reduction are produced in the external medium, any internal acidification must be a result of active proton translocation. However, $TMPD^+/H^+$ antiport as postulated by Cooper and Nicholls (1987) will also lead to internal acidification [cf. Miller et al. (1979)]. Although it is difficult to measure directly the rate of $TMPD^+/H^+$ exchange, kinetic modeling of the steady-state gradients in proteoliposomes allows an estimate of the antiport activity. We believe that significant levels of proton translocation and $TMPD^+/H^+$ activity can both occur in the steady state. Some modeling of this type of system [see Nicholls et al. (1988b) and Cooper (1989)] will be the subject of a forthcoming paper.

Acknowledgments

We thank Peter Rand and Nola Fuller (Brock University) for help with freeze-fracture electron microscopy and Jackie Marsh and Ross Hallett (University of Guelph) for the use of the laser light scattering setup. We also thank John Wrigglesworth (King's College, London) for stimulating discussions.

References

Bayerl, T. M., Schmidt, C. F., & Sackmann, E. (1988) *Biochemistry 27*, 6078–6085.

Casey, R. P., O'Shea, P. S., Chappell, J. B., & Azzi, A. (1984) *Biochim. Biophys. Acta 765*, 30–37.

Cooper, C. E. (1989) Ph.D. Thesis, University of Guelph, ON, Canada.

Cooper, C. E., & Nicholls, P. (1987) *FEBS Lett. 223*, 155–160.

Cooper, C. E., Bruce, D., & Nicholls, P. (1990) *Biochemistry* (preceding paper in this issue).

De Vrij, W., Dreissen, A. J. M., Hellingwerf, K. J., & Konings, W. N. (1986) *Eur. J. Biochem. 156*, 431–440.

Ferguson-Miller, S., Brautigan, D. L., & Margoliash, E. (1978) *J. Biol. Chem. 253*, 149–159.

Hallett, F. R., Craig, T., Marsh, J., & Nickel, B. (1989) *Can. J. Spectrosc. 34*, 63–70.

Herb, C. A., Berger, E. J., Chang, G. K., Morrison, I. D., & Grabowski, E. F. (1987) in *Particle Size Distribution, Assessment and characterization* (Provder, T., Ed.) pp 89–104, American Chemical Society Symposium Series 332, American Chemical Society, Washington, DC.

Hill, B. C., & Nicholls, P. (1980) *Biochem. J. 187*, 809–818.

Kachar, B., Fuller, N., & Rand, R. P. (1986) *Biophys. J. 50*, 779–788.

Kuboyama, M., Yong, F. C., & King, T. E. (1972) *J. Biol. Chem. 247*, 6375–6383.

Madden, T. D., Hope, M. J., & Cullis, P. R. (1984) *Biochemistry 23*, 1413–1418.

Miller, M., Petersen, L. C., Hansen, F. B., & Nicholls, P. (1979) *Biochem. J. 184*, 125–131.

Murphy, M. P., & Brand, M. D. (1987) *Nature 329*, 170–172.

Nicholls, P. (1983) in *Liposome Letters* (Bangham, A. D., Ed.) pp 215–229, Academic Press, London.

Nicholls, P., Hildebrandt, V., & Wrigglesworth, J. M. (1980) *Arch. Biochem. Biophys. 204*, 533–543.

Nicholls, P., Shaughnessy, S., & Singh, A. P. (1987) in *IUB/UNESCO Symposium CYTOCHROME SYSTEMS: Molecular Biology and Bioenergetics* (Papa, S., Chance, B., & Ernster, L., Eds.) pp 391–398, Plenum Press, New York.

Nicholls, P., Cooper, C. E., & Kjarsgaard, J. (1988a) in *Advances in Membrane Biochemistry and Bioenergetics* (Kim, C. H., Tedeschi, H., Diwan, J. J., & Salerno, J. C., Eds.) pp 311–321, Plenum Press, New York.

Nicholls, P., Cooper, C. E., & Wrigglesworth, J. M. (1988b) *EBEC Reports* (Beechey, B., Ed.) Vol. 5, p 119.

Proteau, G., Wrigglesworth, J. M., & Nicholls, P. (1983) *Biochem. J. 210*, 199–205.

Racker, E., & Kandrach, A. (1971) *J. Biol. Chem. 246*, 7069–7071.

Rand, R. P., Kachar, B., & Reese, T. (1985) *Biophys. J. 47*, 483–489.

Singh, A. P., & Nicholls, P. (1986) *Biochem. Cell. Biol. 64*, 647–655.

Wikstrom, M., & Krab, K. (1979) *Biochim. Biophys. Acta 549*, 177–222.

Wrigglesworth, J. M. (1985) *J. Inorg. Biochem. 23*, 311–316.

Wrigglesworth, J. M. (1988) *Mol. Aspects Med. 10*, 223–232.